Materials Science in Additive Manufacturing

REVIEW ARTICLE

Laser additive manufacturing of magnesium alloys and its biomedical applications

Chuyi Liu[1], Chengrong Ling[2], Cheng Chen[2], Dongsheng Wang[3], Youwen Yang[1,2]*, Deqiao Xie[4]*, Cijun Shuai[2,5]*

[1]College of Mechanical and Electrical Engineering, Jiangxi University of Science and Technology, Ganzhou 341 000, China

[2]Institute of Additive Manufacturing, Jiangxi University of Science and Technology, Nanchang 330 013, China

[3]Key Laboratory of Construction Hydraulic Robots of Anhui Higher Education Institutes, Tongling University, Tongling 244 061, China

[4]College of Mechanical and Electrical Engineering, Nanjing University of Aeronautics and Astronautics, Nanjing 210 016, China

[5]State Key Laboratory of High Performance Complex Manufacturing, Central South University, Changsha 410 083, China

Abstract

Biomedical magnesium (Mg) alloy with unique biodegradability and excellent biocompatibility is one of the most sought after materials in medical field for orthopedics applications. Nevertheless, the high corrosion rate and inadequate mechanical properties hinder its development. Apart from that, to obtain the best surgical result, the size and shape of the fixation implant need to be adapted to the individual case. Thus, additive manufacturing (AM) processes, such as laser powder bed fusion (LPBF), are used to overcome these issues. This work reviews the recent advancements in biodegradable Mg-based alloys prepared by LPBF for biomedical applications. The influence of feedstock features and manufacturing parameters on the formability and quality is delineated in detail. The mechanical performances, degradation behaviors, and biological behavior of the LPBF-processed parts are discussed. Furthermore, we also made some suggestions for the challenges of Mg alloys in LPBF processing and applications in biomedical.

Keywords: Magnesium alloy; Additive manufacturing; Biological behavior; Biomedical

***Corresponding authors:**
Youwen Yang
(yangyouwen@jxust.edu.cn)
Deqiao Xie
(dqxie@nuaa.edu.cn)
Cijun Shuai
(shuai@csu.edu.cn)

Citation: Liu C, Ling C, Chen C, *et al.*, 2022, Laser additive manufacturing of magnesium alloys and its biomedical applications. *Mater Sci Add Manuf,* 1(4): 24. https://doi.org/10.18063/msam.v1i4.24

Received: October 30, 2022

Accepted: November 23, 2022

Published Online: December 14, 2022

1. Introduction

1.1. Potential of magnesium in biomedical applications

With the increase in elderly population and the frequent traffic accidents, more and more people are suffering from bone defect[1]. At present, statistics shows that the cumulative number of cases exceeds 20 million in China, with an increment of 3 million new cases every year[2]. The regeneration and reconstruction of damaged tissues have great strategic importance[3]. Medical metal materials, such as titanium alloys, tantalum alloys, and stainless steel, are commonly used as implant to replace the damaged parts in bones due to their excellent mechanical properties and good biocompatibility[4].

However, their elastic modulus and mechanical strength are much higher than natural bone, which cause the "stress occlusion" effect after implantation, thus leading to the atrophy of natural bone tissue and even migration failure[5]. Moreover, they might release some toxic metal ions, which induce inflammation. Unfortunately, the implants do not easily degrade, and thus, they need to be removed in secondary surgery after implantation[6]. In this case, this could the patients will undoubtedly have to endure huge pain and shoulder extra economic burden. Therefore, it is imperative to develop new metal scaffolds for repairing bone defect[7].

Recently, biodegradable metals such as magnesium (Mg), zinc (Zn), and iron (Fe) alloys have become a hot research topic in tissue repair because of their mechanical strength, unique degradation properties, and good biocompatibility[8,9]. After implantation, these biodegradable metals have the sufficient mechanical strength to provide support during the healing process[10]. Importantly, they can be completely degraded *in vivo*, and their degradation products will be metabolized by the human body without any toxic side effects[11]. Compared to Zn and Fe alloys, Mg alloy has received wide attention from experts and scholars since it has the following three significant advantages:

(i) Mechanical compatibility. Mg alloy is a light alloy with low density and high specific strength. Its density (1.8 – 2.1 g/cm^3) and elastic modulus (40 – 45 GPa) are similar to those of human bone, indicating that they can effectively reduce the stress shielding effect[12,13]. It has excellent application prospects in bone tissue defect repair.

(ii) Biodegradability. The standard electrode potential of Mg is −2.37 V. Mg alloy can completely degrade the body by self-corrosion. The degradation products have no apparent side effects on the human body and can be excreted through human metabolic processes[14,15].

(iii) Biocompatibility. Mg, which is involved in synthesizing a variety of proteases and nucleic acids, is one of the essential nutritional elements for humans. Mg ion is conducive to the dilatation of blood vessels and the healing of bone tissue. Therefore, biodegradable Mg alloy is hailed as the new-generation medical metal materials. The comparison between Mg alloy and other bone implants is shown in Table 1.

1.2. Development of Mg-based implants

Mg and its alloys, as the promising implants, are mainly used in bone fixation devices, cardiovascular scaffolds, and tissue engineering scaffolds[20-22]. The advantages of Mg implants and its clinical applications are presented in Figure 1. The development of Mg-based implants has gone through two stages, with the 21st century as the dividing line. Before the 21st century, Mg alloys were mainly used in bone fixation devices. In 1900, Payr *et al.*[23] pioneered the use of Mg as a bone connector for the fixation of injured bone, and the Mg plate produced no adverse effects in animals. In 1906, Lambotte extended the animal *in vivo* experiment to a human clinical study, using Mg plates and steel nails to fix the calf fracture of patients[24]. Still, the Mg plate and steel nails formed galvanic corrosion, which produced a large amount of hydrogen. The implantation site appeared to have a gas swelling phenomenon. In 1938, McBride *et al.*[25] used a bone fixation device made of Mg-Al-Mn alloy to treat multiple fractures, and no negative effects were observed in the fracture tissue after implantation. However, due to the rapid degradation rate of Mg alloy in the human body, the clinical research of Mg alloy as a bone fixation device has stalled in the late 20th century[26].

Due to the rapid development of science and technology after the 21st century, some Mg alloy bone fixation devices have passed clinical trials and obtained regional certification. In 2008, the United States established a research center to study biodegradable biomaterials. In 2013, Syntellix AG successfully developed degradable Mg alloy screws, which passed clinical trials and obtained CE certification[27]. In 2014, the China Food and Drug Administration certified the Mg-Zn-Ca bone nail developed in South Korea because of its relatively slow degradation rate[14]. In recent years, Mg alloys have gradually been used to manufacture cardiovascular and tissue engineering scaffolds. Chaya *et al.*[28] used Mg bone plates and screws and titanium alloy plates and screws to repair bone cracks in rabbits. The results showed that the degradation of Mg bone plate was beneficial to bone healing. Zhao *et al.*[29] used Mg screws to fix vascularized bone grafts with femoral head necrosis and found that released Mg ions could stimulate the generation of fresh bone. Wang *et al.*[30] used Mg-Zn-Y-Nd alloy scaffolds to treat esophageal cancer. The data showed that Mg alloy had good biocompatibility and degradation performance and could kill the esophageal cancer cells.

1.3. Advantages of laser powder bed fusion (LPBF) for the fabrication of implants

To meet the requirements of clinical applications, bone implants should possess not only appropriate mechanical strength and good biocompatibility but also personalized shape to match different damaged parts. The traditional preparation methods of Mg alloy components are mainly casting and powder metallurgy. Although the formed Mg alloy components have good mechanical properties,

Table 1. Comparison of physical performance between Mg alloys and other bone implants

Materials	Density (g/cm^3)	Modulus (GPa)	Compressive yield (MPa)	Elongation (%)
Human bone[12,16,17]	1.8 – 2.1	10 – 30	130 – 180	3 – 6
Mg alloys[16,17]	1.79 – 2.0	37.5 – 65	70 – 140	2 – 11
Ti alloys[17,18]	4.2 – 4.5	79 – 110	795 – 908	6 – 16
Co alloys[17,18]	8.3 – 9.2	220 – 230	450 – 1500	5 – 30
316 L steel[17,18]	8.0	193	172 – 690	12 – 40
Tantalum[17,18]	16.7	188 – 190	138 – 345	1 – 30
Hap[18,19]	3.1	80 – 110	0.03 – 0.3	/
TCP[18,19]	/	24 – 39	2 – 3.5	/
Fe alloys[17-19]	7.8 – 7.9	200 – 205	170 – 690	12 – 40

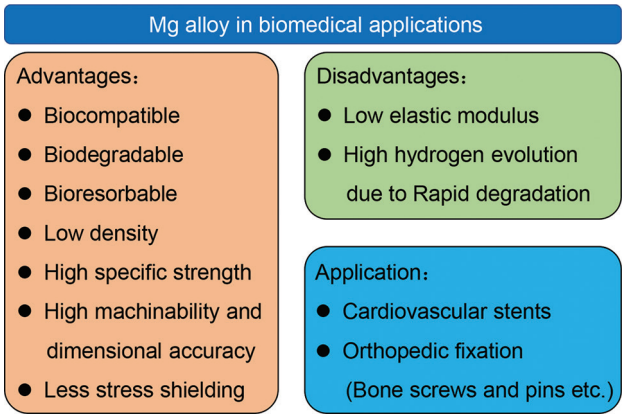

Figure 1. The advantages of Mg implants and its clinical applications.

the process has an extended processing cycle and low material utilization. Unfortunately, these methods cannot easily control the pore size to obtain complex geometric shapes. Additive manufacturing (AM), commonly known as three-dimensional (3D) printing, is a manufacturing technology that integrates computer-aided design, material processing, and molding technologies and uses digital model files as a basis. Meanwhile, through software and CNC systems, special materials are stacked layer by layer in accordance with extrusion, sintering, melting, light curing, or spraying to fabricate block parts[31]. Compared with traditional manufacturing technology, AM could provide a reliable way to obtain personalized complex 3D structures, which can efficiently and reliably replicate anatomical morphology related to tissues and organs. It could prepare precisely controlled pore structure to meet the personalized customization needs of patients. In particular, LPBF is commercially known as selective laser melting (SLM), which uses metallic and non-metallic powders as the raw material[32]. In contrast to other AM technologies, SLM can process a very wide variety of materials. In addition, it is possible to recycle and reuse unmelted metal powder, which allows the efficient use of the material. Due to its characteristics, SLM can be effectively applied as a prospective production technique for valuable materials and components, through cutting down the cost and lead time of fabrication and reducing the loss of material. Therefore, it has attracted increasing interest and attention in fabricating biodegradable Mg-based implants.

In 2011, Ng *et al.*[33] used the SLM process to prepare pure Mg, which was the first report about the Mg alloy for custom biomedical implants. Since then, Mg and its alloys for the degradable implants has become hotspot research in biomedical field. In this review, we present a systematic analysis and discussion on the recent literature on LPBF-processed Mg alloy. In addition, the effect of the comprehensive powder properties, parameters optimization, and post-treatment on their mechanical and degradable properties will be highlighted, along with the current challenges in LPBF-processed Mg alloys. The review also presents insights into the future of Mg alloys and their use in biomedical applications.

2. LPBF-processed Mg alloys

The fabrication of Mg and its alloys through LPBF is deemed to be extremely challenging. On the one hand, due to the inherent inflammability and explosiveness, the preparation conditions of Mg powders are extremely demanding. On the other hand, low evaporation temperature and high vapor pressure of Mg tend to trigger micro-crack during LPBF processing, causing poor structural integrity of parts. Thus, until now, there is no relevant report on LPBF-processed ultrapure Mg (>99.9%). A great deal of current research on Mg prepared by LPBF has focused on its alloys. This is due to their good workability and low risk.

2.1. Preparation of the feedstock

It is well known that LPBF is a typical powder metallurgy technology. Powder properties are an essential part of the LPBF industry chain. The powder should possess a

spherical morphology to form a homogeneous layer of continuously deposited powder. This feature is vital to improve the flowability and packing density. At present, the methods for preparing Mg alloys powder mainly include water, gas, and plasma atomization, plasma rotating electrode (PRE) atomization, and evaporation-condensation. Among them, aerosolization is widely used for the preparation of Mg powder for LPBF processing with a particle size distribution between 20 and 70 μm. Moreover, the sphericity of the powder can reach 98%. Usually, high sphericity means superior flowability, which is conducive to powder spreading with scraper and as-built parts with high quality.

2.1.1. Water atomization

Water atomization is an atomization method that uses water as the atomization medium to break the molten metal. The advantages of water atomization include simple equipment structure, high efficiency, and low atomization cost. However, the disadvantage of water atomization is that the prepared powder has high impurity and poor sphericity. It was due to the fact that the reaction between active metal and atomization medium at high temperature increases oxygen content. In addition, the metal droplets formed by water atomization breaking in the rapid solidification stage are irregular due to the large specific heat capacity of water.

2.1.2. Gas atomization

The aerosolization method uses high-speed airflow to crush the liquid metal stream, forming tiny droplets, and then quickly condensing to obtain the formed powder. Compared with water atomization, gas atomization uses inert gas (i.e., argon and nitrogen) as atomization medium. The metal prepared by this method has the advantages of small powder (particle size <150 μm), uniform composition, and high sphericity. Gas atomization is suitable for producing most metals and alloys, which is the primary production method for spherical metal powders in AM processing. At present, most of the powder is produced and prepared by the gas atomization method, accounting for 30%–50% of the powder produced in the world[29]. The density and microstructure of 17-4PH stainless steel parts prepared from gas-atomized and water-atomized powders were comprehensively investigated by Irrinki *et al.*[34]. The morphology of water-atomized powder and gas-atomized powder is shown in Figure 2.

2.1.3. Plasma atomization

Plasma atomization was reported by Entezarian *et al.* in 1996 for the production of highly spherical powders with an average particle size of 40 μm[36]. This approach uses the

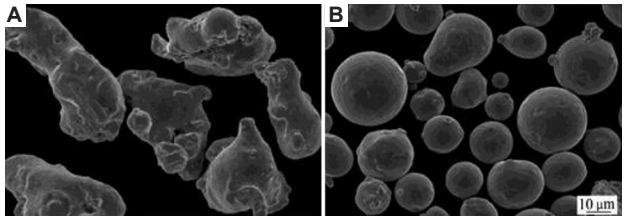

Figure 2. The SEM image of (A) water-atomized powders and (B) gas-atomized powders[35].

focused argon plasma jet generated by a plasma torch to melt the wire as initial material, which then results in the formation of tiny metal droplets. The plasma torch produces an extremely high-temperature argon plasma, which can inhibit the rapid solidification of molten and superheated metal droplets into irregular shapes[36]. Therefore, the droplets spend sufficient time in the superheated state and adopt an equilibrium shape (ideal spheres) driven by the surface tension during the falling process. The atomization and condensation process of the metal powder is carried out in an inert atmosphere.

2.1.4. Plasma rotating electrode atomization

Plasma rotating electrode (PRE) atomization is a centrifugal atomization process. It uses the plasma arc generated by a plasma gun as a high-temperature heat source to melt the raw material, which is in the form of an electrode rod and rotate at approximately 15,000 rpm. Meanwhile, centrifugal force separates the molten material from the rod, which then results in the formation of tiny metal droplets. The metal droplets solidify into spherical powders before they hit the chamber walls. This method was invented to reduce the volume of gas consumed to prepare each unit weight of atomized powder, as well as to address the generally low yield of fine powders prepared by conventional gas atomization processes. Notably, the yield for the process was closely related to this centrifugal force, that is, the rotation speed. In addition, the process can eliminate the risk of ceramic contamination due to melting of reactive metals in ceramic crucibles, thus obtaining high-purity spherical metal powder. Zheng *et al.*[37] reported that Mg-15Gd-0.4Zr (wt%) alloy powders with the size ranging from 75 to 250 μm were prepared by PRE atomization. As compared with aluminum (Al) powder prepared by gas atomization, it exhibited relatively high sphericity, as shown in Figure 3. The Mg alloy powder was adopted as the base material, and corresponding samples were successfully prepared by laser-directed energy deposition.

Based on the above description, the powder preparation methods are capable of producing spherical powders tailored for AM process. Recently, the rapid development of AM significantly increased the demand for spherical

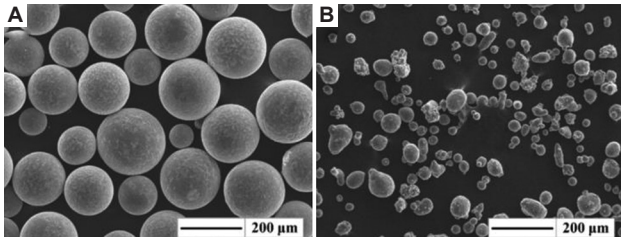

Figure 3. Morphology of (A) the pre-atomized Mg-15Gd-0.4Zr (wt%) alloy powder and (B) the gas-atomized Al powder.

metal powders in the market. The efficient preparation of high-quality spherical metal powders is vital to promote AM technology upgrades and industrial applications. Therefore, the existing powder preparation methods need to be improved. For the gas atomization method, optimizing the structure of the atomizer and improving the kinetic efficiency of the atomized gas are the most effective means to improve the quality and production efficiency of metal powders. For the PRE atomization method, to efficiently prepare high-quality spherical powders, the rotation speed of the electrode bar is increased, while the reasonable plasma heat source and power are also fed.

2.2. Parameters optimization

The performance of SLM prepared product strongly depends on the processing parameters, such as laser power, scanning speed, hatch spacing, and layer thickness. The previous studies have shown that the process parameters are considered appropriate when the following requirements are fulfilled in scanning tracks and layers[38]: (π) The scanning tracks should be continuity, (θ) each layer has to be high enough to build up the part cumulatively, (ρ) every layer should be high enough, and (σ) the connection angle between two adjacent layers should be close to 90°.

2.2.1. Laser power

High laser power can improve the wettability of the molten pool and provide more power for powder consolidation. Ji *et al.*[39] reported an analytical model to predict the grain size of the part after LPBF process. Results show that the maximum surface temperature of the component is not influenced by the scanning speed. In addition, the average grain size reduced with the increasing of laser power. He *et al.*[40] prepared AZ61 alloy with a relative density of 98%. The forming zone of AZ61 with input laser power from 60 W to 90 W was determined. The results show that the increase in laser power helps improve the densification of the material and the formation of equiaxed grains, thus improving the resistance to degradation and microhardness. However, too high laser power can lead to grain coarsening and a decrease of Al solid solution in the Mg matrix, resulting in increased mass loss and decreased microhardness.

2.2.2. Scanning speed

The appropriate scanning rate can increase the heating time of metal powder. The fabrication of compact component can be achieved with low scanning speed, as it allows longer contact time between powder and laser, thereby increasing the rate of energy transfer to the powder bed. With the scanning speed increasing, less energy is transferred to powder, which always results in incomplete melting of the particles. Shuai *et al.*[41] reported the influence of SLM processing parameters on the corrosion performance of ZK60 alloy. At an energy density of 600 J/mm^3, the final as-built part with a relative density of 97.3% was obtained. Spierings *et al.*[42] analyzed the impact of different laser scanning speeds on the static mechanical properties of SLM-treated scandium (Sc) and zirconium (Zr)-modified Al-Mg alloys. The results showed that the scanning speed could affect the hardness and mechanical performance of the alloy, while yield strength was barely affected by the laser scanning speed.

2.2.3. Laser energy density

Although the variety of laser powers or scanning speeds can significantly influence the forming quality and performance of AM-processed part, it is difficult to describe their effects individually. An empirical formula for evaluating the input energy of laser additive using laser energy density[43] is given below:

$$E_V = \frac{P}{V.H.D}$$

Where, E_v represents energy density (J/mm^3), P is the laser power (W), V is the scanning speed (mm/s), H is the hatch spacing (mm), and D is the layer thickness (mm). After forming, the forming quality of samples is measured by density and surface roughness. In general, the surface of the sample with high density is relatively flat and has a low surface roughness, as shown in Figure 4. In the case of low laser energy density, the temperature in the molten pool is also relatively low so that the metal powder cannot be fully melted, and noticeable unmelted powder particles and a large number of pores can be observed between the adjacent molten layers, which result in low density. When the laser energy density is too high, the temperature in the molten pool easily exceeds the boiling point of magnesium powder because the melting and boiling point of magnesium powder is relatively close, resulting in a large amount of powder evaporation, which leads to the formation of local vapor pressure, powder splashing phenomenon, and formation of a large number of pores, as displayed in Figure 5.

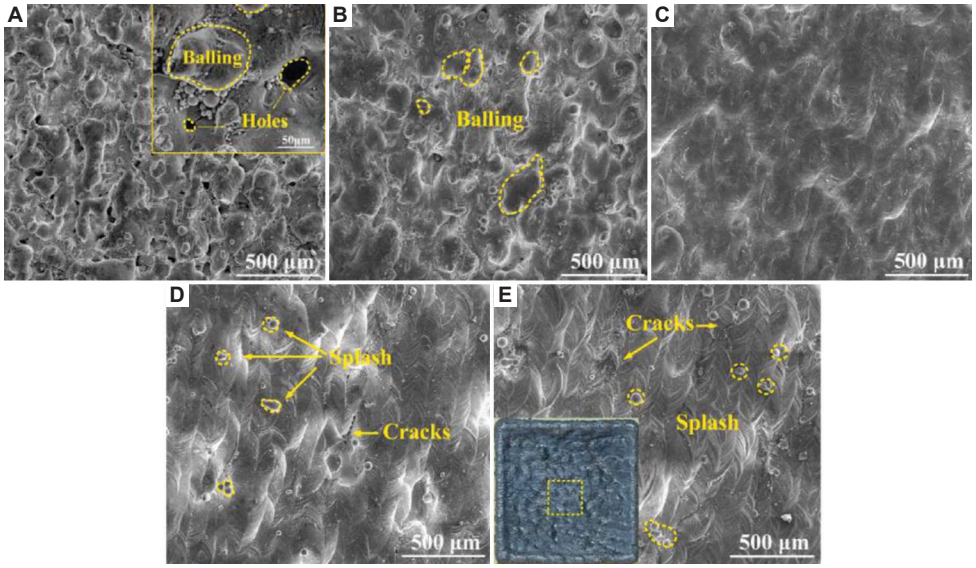

Figure 4. (A-E) SEM images of SLMed ZK60 alloy surface morphologies at different energy density[44].

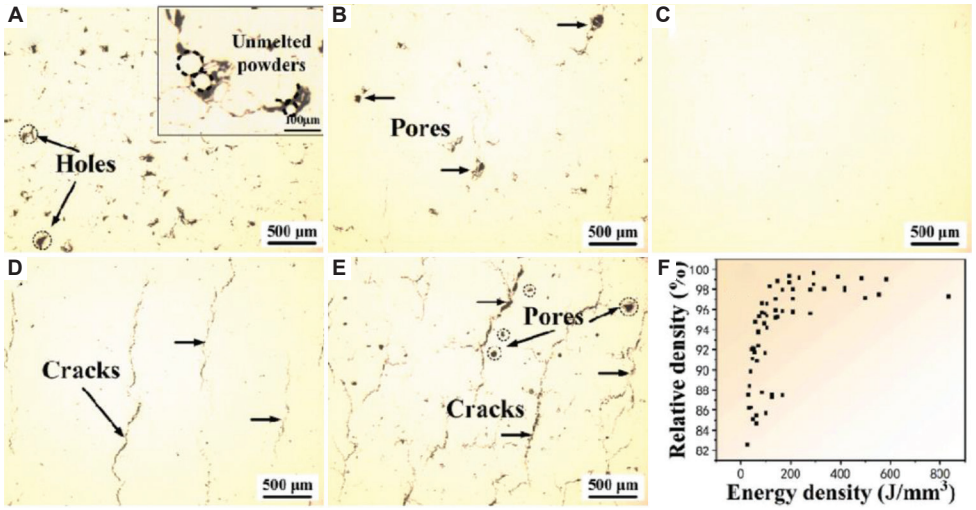

Figure 5. (A-F) Optical micrographs of the SLMed ZK60 Mg alloy at different energy density[44].

Esmaily *et al.*[45] reported the influence of laser energy density on the forming quality of WE43 magnesium alloy by changing the laser power and scanning rate and obtained the sintering process window diagram. WE43 has many pores and unmelted metal powders in the low-energy density region, resulting in a very low material density and poor mechanical properties. In the high-energy density area, due to the high temperature, there is apparent burning and evaporation phenomenon, resulting in the keyhole and other phenomena, and the forming quality is poor. The stable molten pool can only be obtained under the appropriate laser energy density in the forming area, which ensures good forming quality and dimensional accuracy and achieves 98.3% density.

Wei *et al.*[46] studied the influence of different laser energy densities on the forming properties, microstructure, and mechanical performance of AZ91D samples. They found that the forming parts with high density and no obvious macroscopic defects could be obtained between 83 and 167 J/mm^3. When the laser energy input is over 214 J/mm^3, the sample cannot be deposited due to solid evaporation, and there is a severe burning phenomenon. When the laser energy input is <77 J/mm^3, the powder cannot be completely melted, resulting in many holes in the sample. Therefore, only in the appropriate processing window can high-density parts be prepared. The optimization parameters obtained from the current literature are collated in Table 2.

Table 2. Additive manufacturing process parameters for magnesium and its alloy

Material	Laser power (W)	Laser spot size (μm)	Scanning speed (mm/s)	Layer thickness (μm)	Hatch spacing (μm)
Mg[47]	100	50	10	100	/
Mg-xZn[48]	70	50	100	100–200	/
AZ61[49]	150	70	400	40	60
AZ91D[46]	200	/	500	40	90
ZK30[48]	75	150	15	50	50
ZK60[41]	50	150	8	100	100
ZK60-xCu[48]	60	150	10	/	100
Mg-Ca[50]	80	10	/	40	150
ZK60-BG[51]	80	140	/	60	60
ZK61[52]	100	/	100	40	1500
WE43[45]	280	1200	/	30	40
GWZ1031K[53]	80	200	/	30	100

2.3. Post treatments

SLM, as a typical AM technology, can reliably prepare Mg-based products, which especially own complex geometries and do not require molds and accessories[54]. Besides, it also possesses these advantages, such as small machining allowances and high material utilization. Notably, Mg is susceptible to oxidation due to its high chemical reactivity and relatively low melting and boiling points to cause high evaporation during melting[55,56]. Therefore, SLM-processed Mg alloy parts exhibit many defects such as high surface roughness, porosity, residual stresses, anisotropy, and undesired microstructures, which can greatly reduce the overall performance of the parts. The removal of the defects is of great practical importance, where some post-treatments are commonly performed, especially hot isostatic pressing (HIP) and calcium hydrogen phosphate dihydrate (DCPD).

2.3.1. Hot isostatic pressing (HIP)

HIP is a frequently used thermomechanical treatment method that eliminates the porosity and relieves the residual stresses, thus improving ductility, fatigue resistance, and microstructure. The method is performed under high-temperature and -pressure conditions, in which the temperature and pressure usually reach 1000 – 2000°C and 200 MPa, respectively. The working pressure generated by a high-pressure inert gas in a closed vessel is close to the yield point of the as-built parts, thus causing plastic deformation. The parts are pressed evenly in all directions with high temperature and pressure, which eliminates these defects to form a dense and uniform microstructure. Therefore, the treated parts can show high density, good uniformity, and excellent performance. Esmaily *et al.*[45] processed WE43 Mg alloy through SLM and found that HIP treatment is an effective method to eliminate the processing defects, thereby obtaining almost fully dense parts, as shown in Figure 6. Gangireddy *et al.*[57] showed that at higher initial porosity, HIP treatment was beneficial for the densification of LPBF formed WE43 magnesium alloys, but could not improve the densification of samples with smaller porosity due to the closed nature of the pores. The cooling rate of laser AM is much higher than that of traditional casting, and an excessively fast cooling rate may be detrimental to the precipitation of strengthening phases. A large amount of residual stress caused by excessive cooling rate, texture, and mechanical anisotropy generated along the direction of heat flow can be eliminated by heat treatment[58].

2.3.2. Calcium hydrogen phosphate dihydrate (DCPD)

The surface roughness of as-built parts affects the mechanical properties and degradation rate. Coatings can modulate the degradation behavior and improve the biological properties. Wang *et al.*[59] applied DCPD to the surface coating of JDBM porous scaffolds with helical tetrahedral structural units, as shown in Figure 7. DCPD treatment slowed down the degradation rate of the scaffolds and improved their biocompatibility. Dou *et al.*[60] used the sol-gel impregnation method to prepare 45S bioactive ceramic coatings on AZ31 Mg alloy substrates and found that the corrosion resistance was significantly improved. Rojaee *et al.*[61] synthesized hydroxyapatite coating on AZ91 alloy by electrophoretic deposition process, which significantly improved its corrosion resistance and biological properties. Razavi *et al.*[62] prepared nanostructured magnesite and diopside coatings by electrophoretic deposition, which also improved the corrosion resistance and biological activity of magnesium alloys. Kopp *et al.*[63] used plasma electrolytic oxidation (PEO) to treat the surfaces of WE43 Mg alloy scaffolds with different pore sizes prepared by

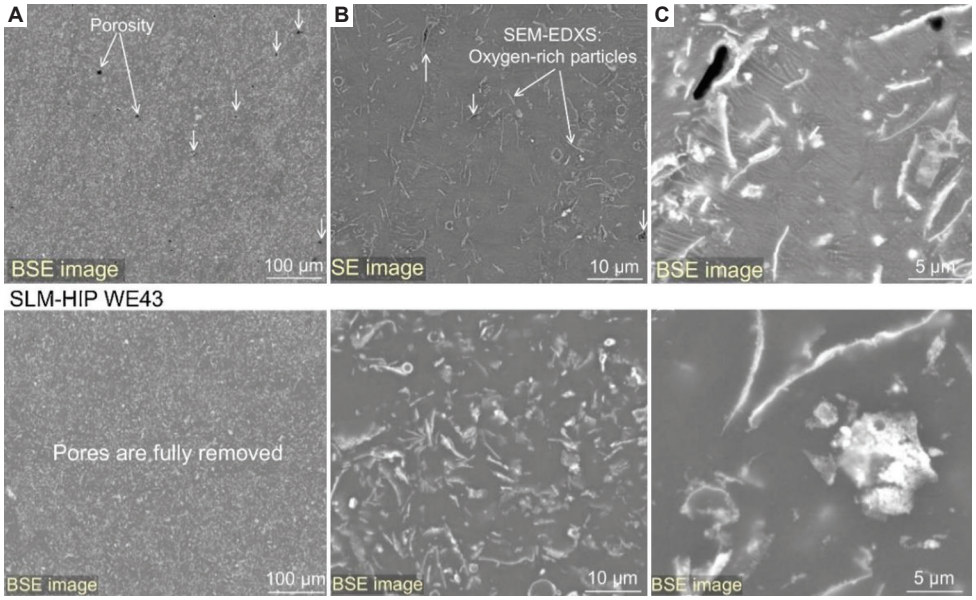

Figure 6. (A-C) BSE-SEM micrographs revealing the microstructure of the sample in the SLM-prepared WE43 with and without HIP treatment.

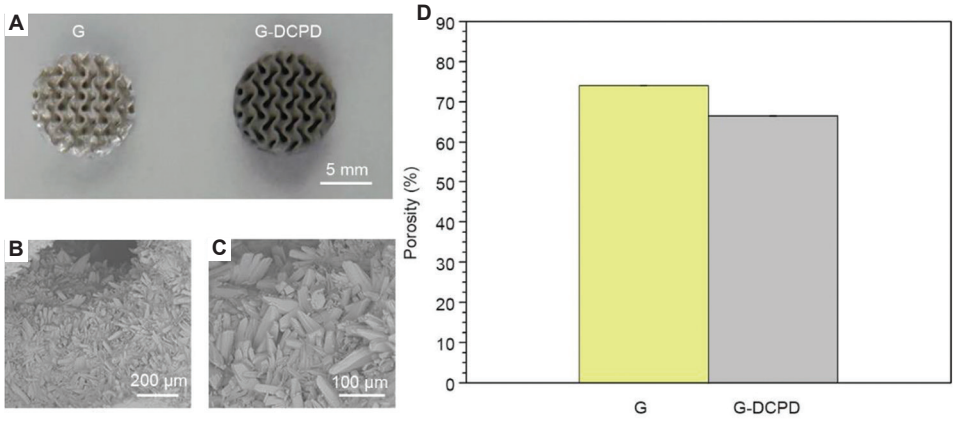

Figure 7. (A) Macrograph, (B and C) SEM, and (D) porosity of the G-DCPD scaffold.

LPBF technique. The results showed that PEO significantly reduced the degradation rate of the scaffolds at the initial stage of DMEM soaking. After soaking for 21 days, the stability of the PEO-modified surface decreased, and the weak parts were eroded and cracked.

2.3.3. Friction stir processing

In recent years, severe plastic deformation (SPD), which is an emerging technology, has been widely used to the post-treatments of SLMed parts. Friction stirring processing (FSP) is a typical SPD technique, with its basic principle derived from friction stir welding (FSW), as shown in Figure 8. It is able to simultaneously use high strains, high strain rates, and high temperatures to fully move the material, which results in grain refinement, second phase fragmentation,

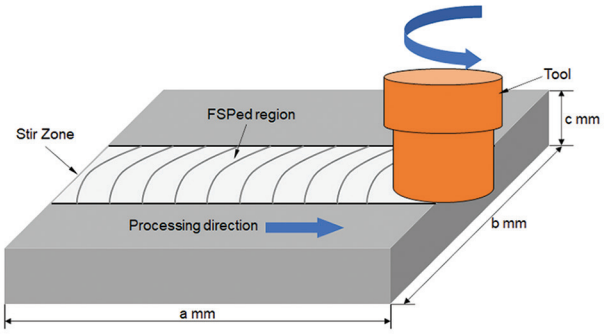

Figure 8. Schematic diagram of friction stirring processing.

homogenization, and densification within the stirring zone[64]. Huang *et al.*[65] used FSP to reduce the porosity and

homogenize the microstructure of the SLMed Ti_6Al_4V alloy, the results showed that fracture strain increased from 0.21 to 0.65 after FSP. In addition, FSP improves the ductility and fatigue life of the SLMed-$AlSi_{10}Mg$ alloy, due to the spheroidization of the eutectic phase, the homogenization of the microstructure, and the reduction in porosity[66]. However, to the best of our knowledge, there are only a very limited number of studies relating to the adjustment of the microstructure and enhanced mechanical properties of SLMed-Mg alloys by FSP. Deng *et al.*[67] found that FSP treatment of SLMed-Mg alloys resulted in a reduction of porosity from 0.779% to 0.015%, disappearance of melt pool boundaries, columnar to equiaxed transformation, and grain refinement, which significantly improved the mechanical properties of the Mg-Gd-Zr alloy.

2.3.4. Laser beam polishing

Laser polishing is an efficient, non-contact, and fully automated post-treatment technology that provides excellent performance in reducing the surface roughness of SLMed parts. In the past two decades, laser polishing has been widely used to reduce the surface roughness of polymers, metals, ceramics, and other materials. In contrast to conventional polishing processes, laser polishing smoothens rough surfaces using thermal energy to melt a thin layer of material, as shown in Figure 9. In laser polishing, a precisely controlled laser beam is guided onto the surface of the part for polishing. By controlling the energy of the laser beam, the peak on the surface is just melted, and the molten metal is generated due to the multi-directional surface tension and gravity, and then, it is filled into the valley. In this case, there is no material loss during laser polishing. The laser power, spot size, and scanning speed are the main control parameters to obtain a smooth surface[68]. At present, laser polishing has demonstrated its ability to polish various materials, from reflective materials such as aluminum to high strength materials such as Inconel and titanium alloys[69]. Unfortunately, there are no relevant reports on laser polishing for SLMed Mg alloys.

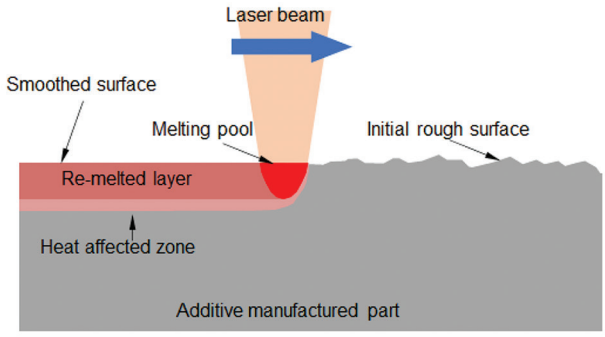

Figure 9. Schematic diagram of laser beam polishing.

3. Performance of LPBF developed Mg alloys

3.1. Mechanical properties

An ideal orthopedic implant should have sufficient mechanical strength and excellent stress conduction capability, matches with the surrounding bone tissue, and provides mechanical support during the healing process of bone tissue. Processing method directly affects the mechanical properties of Mg alloys. Compared with cast Mg alloys, due to the influence of grain refinement, solid solution strengthening, and other factors, the mechanical properties of Mg alloys manufactured by laser AM have been improved to varying degrees in various aspects. The mechanical properties of bone are closely related to age, bone health, and bone type. Zhang *et al.*[70] prepared porous Mg scaffolds with porosity of 33 – 54% using fiber deposition hot pressing technology, and their Young's modulus and compressive strength were comparable to those of human cancellous bone.

Hyer *et al.*[71] used LPBF to prepare a dense WE43 alloy. Under the compressive action, the average yield strength of the newly built WE43 structure was 224 MPa, the compressive strength was 417 MPa, and the failure strain was 9.5%. Under tension, the newly constructed LPBF WE43 has an average yield strength of 215 MPa, a tensile strength of 251 MPa, and a failure strain of 2.6%. A study by Fang *et al.*[72] on the mechanical properties of hot rolled and WAAM-GTA prepared AZ31 samples showed that the performance of WAAM-GTA AZ31 along the direction of travel was always better than that along the build direction. Whether there were large pores within the specification length of the processed tensile samples, its mechanical properties will vary. Deng *et al.*[53] systematically analyzed the effect of different solution conditions and aging heat treatment on the microstructure and mechanical properties of SLM GZ112K alloy. Appropriate post-heat treatment is an effective measure to improve the microstructure and mechanical properties of SLMed alloy. SLM-T6 alloy meets the requirements of high tensile strength, SLM-T4 alloy meets the requirements of high ductility, and SLMed alloy achieves a good combination of tensile strength and ductility. The ultra-high yield strength of SLM-T6 GZ112K alloy mainly comes from the following four aspects: Fine-grain strengthening with average grain size <3.1 μm, precipitation strengthening of β′-aging precipitation, secondary phase strengthening of long-period stacking-ordered (LPSO) structure and X phase, and the extra composite strengthening from the coexistence of basal and prismatic precipitates. Wang *et al.*[73] studied the effect of geometric design on the dynamic response of additively fabricated Mg scaffolds, and the results showed that geometric design had a significant effect on

the compression fatigue performance of Mg scaffolds. A summary of the mechanical properties of the additively manufactured biodegradable Mg alloys from the literature is presented in Table 3.

3.2. Degradation performance

The previous studies have shown that AM prepared Mg and its alloys possess fine grain size and homogeneous microstructure, which can obtain lower degradation rates, mainly due to improved passivation properties and reduced micro-galvanic corrosion[77]. Despite that, their corrosion rate in the body fluid environment is still unable to meet the needs of bone implants. For an ideal biodegradable bone metal implant, they have a corrosion rate of <0.5 mm/year and need to provide mechanical support for 12 – 24 weeks to meet the clinical requirements[78,79]. This means that the AM-processed biodegradable Mg and its alloys implants need to be regulated. The corrosion resistance of the additively manufactured Mg and its alloys in the current studies is summarized in Table 4.

3.2.1. Scavenging effect

Many impurities, such as iron, nickel, and copper, in Mg and its alloy commonly exhibit relatively high potential. This causes the micro-galvanic corrosion with matrix and thus increases their degradation rate. In this case, the corrosion resistance of Mg alloys can be significantly improved by adopting high purification methods or reducing the impurity concentration by improving the processing technology. Han *et al.*[80] found that the degradation rate of high purity Mg *in vivo* was much lower than that of Mg-containing iron impurities. Cao *et al.*[81] slowed down the corrosion rate of Mg alloys by adding a certain amount of Zr to the molten Mg alloy to remove the impurity iron. Studies have shown that Zr and iron can easily form a precipitate phase, which precipitate at the bottom of the melt, thereby achieving purification effect. Peng *et al.*[82] used a zone solidification method to prepare Mg alloys and found that the corrosion rate of the alloys purified by this method was lower than that of conventionally cast Mg alloys.

3.2.2. Alloying treatment

Alloying treatment is an effective way to improve the corrosion resistance of Mg alloys by changing the microstructure and the type of precipitates. At present, researchers have developed a series of biological Mg alloys by alloying methods, and their properties have been studied. Shuai *et al.*[83] found that with the increase of Al content, α-Mg dendrites and intermetallic compounds

Table 3. Mechanical performances of the LPBF-manufactured biodegradable Mg alloys

Type			Mechanical properties	Improvement mechanisms
Shapes	Materials	Dimensions		
Block	ZK60[41]	Cubic 6 × 6 × 6 mm³	Microhardness: 89.2 Hv	High densification, fine-grain strengthening, and solution strengthening
	AZ91D[46]	Bone-shaped gauge 25 × 6 × 2 mm³	UTS: 296 MPa, UYS: 254 MPa Microhardness: 100 HV	Fine-grain strengthening
	AZ61[49]	Bone-shaped gauge 25 × 6 × 1.5 mm³	UTS: 287.1 MPa, UYS: 233.4 MPa, EL: 3.12%	Fine-grain and solid solution strengthening
	GWZ1031K[53]	Bone-shaped gauge 18 × 3 × 10 mm³	UTS: 347 MPa UYS: 310 MPa EL: 4.1%	Fine-grain strengthening
	Mg-8Zn[74]	Cuboid 5 × 5 × 3 mm³	Hardness: 71.5 Hv	Fine-grain strengthening
Porous	Mg-Ca[50]	Cuboid 6 × 6 × 9 mm³	UCS: 111.19 MPa Elastic modulus: 1.26 GPa	Optimizing the laser parameters
	ZK61[52]	Cuboid 6 × 6 × 9 mm³	Microhardness: 106.75 Hv UCS: 50.95 MPa Elastic modulus: 0.91 GPa	Fine-grain strengthening, solution strengthening, and precipitation strengthening
	WE43[75]	Cylindrical D (6 mm), H (6 mm)	Hardness: 77.41 Hv UCS: 21.21 MPa Elastic modulus: 0.79 GPa	Optimized structure of porous units
	WE43[76]	Cubic fluorite	UCS: 71.48 MPa	Optimized structure of porous units

Table 4. Corrosion resistance of the LPBF-manufactured Mg and its alloys

Material	Soaking time	Degradation behaviors
Mg[47]	1 day	pH in SBF: ~10.5
Mg-6Zn[74]	7 day	Evolved H_2 volume in SBF: 32.2 mL/cm^2
ZK60[41]	2 day	H_2 volume evolution rate in SBF: 0.006 mL/cm^2/h
ZK60-0.2Cu[92]	7 day	pH in SBF: 9.49 CR in SBF: ~1.01 mm/year
ZK60-BG[51]	7 day	CR in SBF: 0.51 mm/year
WE43[45]	20 h	CR in 0.1 M NaCl solution: 5 mm/year
Amorphous Mg-Zn-Ca[88]	/	CR for current density in SBF: 0.35 mm/year

SBF and CR represent simulated body fluid and corrosion rate, respectively

were effectively refined. Li *et al.*[84] reported that Zn addition refined the grain size to promote the formation of passivation films on the substrate, thus providing effective protection for the Mg substrate. Luo *et al.*[85] found that the alloying of rare earths significantly reduced the proportion of β phase and promoted the formation of γ phase with a larger active potential, which reduced the micro-galvanic corrosion with the Mg matrix. In addition, the introduction of alloying elements improves the stability or structural integrity of corrosion product layer on the substrate surface with strong protective ability. Leleu *et al.*[86] introduced alloying element Y into Mg alloys, which formed a dense surface film after immersion in chloride rinsing solution and played a significant protective role. Willbold *et al.*[87] added rare earth elements (La, Nd, and Ce) to Mg matrix and found that the rare earth oxides formed on the surface of the Mg alloy to improve the passivation ability of the surface film. Notably, most of rare earth elements have low solid solubility in Mg matrix, thus excessive addition of rare earths can cause galvanic corrosion to accelerate the degradation and bring about cytotoxicity problems.

3.2.3. Amorphous alloy

Amorphous alloy, also known as metallic glass, is a non-equilibrium metal material with excellent corrosion resistance. Wang *et al.*[88] prepared $Mg_{60}Zn_{33}Ca_7$ amorphous alloy by melt spin quenching method. The corrosion potential shifts positively and the corrosion current density decreases, thus showing excellent corrosion resistance. Chen *et al.*[89] reported the research on Mg-based amorphous alloys, which were processed by traditional copper mold casting process. The amorphous alloys possess great glass forming ability, high fracture strength and surface hardness, and good plasticity. Zhang *et al.*[90] prepared Mg-based amorphous alloys by rapid cooling. The results show that the corrosion resistance of the amorphous alloy is obviously better than that of the crystalline alloy with the same composition. Zberg *et al.*[91] also studied the degradation process of Mg-Zn-Ca amorphous alloy as a biodegradable medical material and found that the corrosion resistance was significantly improved. Moreover, there was no obvious hydrogen evolution reaction during the degradation process.

3.3. Biological behavior

Medical implants need to have excellent biocompatibility to avoid toxic effects on the human body[93]. At present, there are little reports on the biocompatibility of additively manufactured metal implants. The biocompatibility evaluation of Mg-based degradable metals for AM is still at the cellular and *in vitro* levels. The factors affecting biocompatibility are mainly its chemical properties and degradation products. Ouyang *et al.*[94] reported that the large pores of the metal scaffolds were favorable for nutrient supply, while the small pores were favorable for cell growth.

Bioactive ceramics have excellent osteoconductive and bioactivity. Rojaee *et al.*[95] synthesized hydroxyapatite coating on AZ91 alloy by electrophoretic deposition process, and its corrosion resistance and biological properties were significantly improved. Razavi *et al.*[62] prepared nanostructured magnesite and diopside coatings by electrophoretic deposition, which also improved the corrosion resistance and bioactivity of magnesium alloys. Tian *et al.*[96] used ammonium bicarbonate particles as a pore-forming agent, and then prepared porous Mg scaffolds by powder metallurgy process, and coated bioactive ceramics on the surface of Mg scaffolds in a low vacuum environment. The results showed that the coated Mg scaffolds have obvious biological activity, and the coating effectively delays the degradation rate of magnesium stents and improves its mechanical integrity.

Rahimi *et al.*[97] successfully prepared chitosan and nanofiber coatings on the surface of AZ31 Mg alloy by anodizing combined with electrospinning. The coating not only has good corrosion resistance but also has good cell adhesion and proliferation ability. However, due to the large differences in physical properties and mismatched degradation rates, the surface coating is easy to crack or even falls off after implantation, making it difficult to achieve long-term effective protection. Dutta *et al.*[98] prepared Mg/bioglass composites by microwave sintering, and the results showed that the corrosion resistance, mechanical properties, and biocompatibility were

improved. Obviously, the introduction of bioactive ceramics can not only induce the formation of calcium and phosphorus layers, providing long-term stable protection, but also greatly improve the biological performance.

Recently, the use of mesoporous bioglass as a reinforcing phase to prepare Mg-based composites for bone repair has been proposed. Mesoporous bioglass has uniform and ordered mesoporous channels (2 – 50 nm) and high specific surface area (500 – 800 m^2/g)[99]. More importantly, as a silicon-containing active ceramic, a large number of silanol groups will be formed on the interface at the initial stage of degradation, thereby forming a negatively charged silica gel layer. Under alkaline conditions, the silica gel layer acts electrostatically to adsorb Ca^{2+} and HPO_4^{2-} in the solution, thereby inducing *in situ* deposition of apatite. *In vitro* degradation tests showed that this *in situ* deposited calcium-phosphorus layer effectively enhanced the biological activity of Mg alloy substrates.

4. Challenges for the future

4.1. Challenges of LPBF-processed Mg Alloys

Due to the inherent characteristics of Mg alloys such as low evaporation temperatures, high vapor pressures, and a high propensity to oxidize, the manufacture of degradable Mg-based implants through AM presents a great number of challenges.

(i) The preparation of Mg powder that can be used for AM processing and degradable Mg-based implants is difficult. The preparation conditions of Mg powders are extremely demanding and the slightest inadvertence can lead to explosive accidents. Moreover, in the current market, the Mg alloy powders commonly used in AM processing are pure Mg, AZ91D, and WE43 powders. Due to the biological toxicity of Al element, AZ91D alloy contains 9% (mass fraction) of Al; therefore, only pure Mg and WE43 powders are suitable for degradable Mg-based implants.

(ii) The AM processing for Mg alloys always produces severe powder splashes due to low evaporation temperature and high vapor pressure of Mg alloys, and this phenomenon is very different from AM processing steel, Ti, or Al. Powder spattering can significantly reduce the stability of the Mg alloy during AM processing, as some Mg powder is removed by steam along the scan path, where defects are likely to occur in subsequent scan passes. In this case, a strategy of powder replenishment is necessary for Mg alloys during AM processing. However, there are no relevant studies on the interaction between Mg powder evaporation, gas flow, and laser input.

(iii) The quality of components prepared by LPBF is difficult to maintain consistently. Due to the complexity of the process chain, many potential fluctuations may occur during manufacturing process, which leads to variable quality of LPBF parts. Recently, a large number of scholars have explored the use of machine learning (ML) algorithms to overcome this obstacle using datasets obtained at various stages of the LPBF process chain[100]. Before LPBF, ML algorithms can be used for part design and document preparation. During the LPBF process, ML can be applied for process parameter optimization and *in situ* monitoring[101]. In addition, ML can also be integrated into post-processing. Therefore, in the future, it is promising to attempt to integrate ML algorithms into different stages of the LPBF process chain to better control the quality of LPBF Mg alloys.

4.2. Challenges of Mg alloys in biomedical applications

In the early stage, most of the medical Mg alloys were in the basic research stage, and the types of alloys that can be clinically applied are rare. At present, there are only high-purity Mg and WE43. Other Mg alloys still face great challenges in clinical applications, including the following problems.

(i) The degradation rate is too fast. Since the electrode potential of magnesium is −2.37 V, it usually appears as an active anode. Corrosion reaction occurs in the body fluid environment, and more $Mg(OH)_2$ is generated on the Mg matrix. The corrosion layer has a loose structure and poor corrosion resistance. In addition, bodily fluids contain a large amount of Cl^-, which will further react with $Mg(OH)_2$ to form the more soluble $MgCl_2$, thereby accelerating the degradation rate.

(ii) The mechanical strength and toughness are insufficient. For materials used in bone fixation and support, high strength and moderate plasticity are required, such as yield strength ≥300 MPa and elongation ≥10%; and for materials used in coronary stents and balloon dilators, high plasticity and medium strength are required, such as elongation ≥20% and yield strength ≥150 MPa. Mg alloys are difficult to enhance plasticity with increasing strength.

(iii) Biocompatibility verification is insufficient. Mg has good biocompatibility, but other alloying elements are inevitably added in the smelting process, which is potentially toxic to the human body. For example, Al can cause chronic neurotoxicity and lead to Alzheimer's disease; some rare earth elements (Y, Nd, Pr, etc.) are potentially toxic after implantation. The corrosion process will be accompanied by the production of a large amount of OH^- and H_2, which can easily trigger an inflammatory response.

Usually, the regeneration cycle of bone tissue is very long, and the implant needs to remain in the body for about 6 – 12 months to fully the reconstruct bone tissue. Bone healing goes through three necessary stages: Inflammation, repair, and bone remodeling. In the first two stages, the bone defect site cannot bear weight, and implants are needed to provide sufficient support to prevent secondary injury. Therefore, in the early stage of healing, Mg alloy implants are required to have high mechanical strength to provide sufficient support; at the same time, a low degradation rate must be maintained to maintain the integrity of the mechanical structure and prevent mechanical failure due to excessive degradation. In addition, it can avoid problems such as swelling and local alkalinity caused by the production of a large amount of H_2, which results in inflammation of the implantation site. Therefore, improving the corrosion resistance of Mg alloys has become a top priority.

5. Conclusions

This paper reviews the research progress in the field of laser AM of Mg alloys, and summarizes and compares their powder preparation, process parameters, and post-processing. Biological Mg alloys show great application potential in the field of tissue engineering due to their good mechanical properties, natural degradability, and biocompatibility. However, under the complex human physiological environment, the corrosion rate cannot be effectively controlled. The follow-up research can start from the following aspects:

(i) Further studying the influence of alloying elements on the mechanical properties of Mg alloys, analyzing the changing trend of the mechanical properties of magnesium alloys during the corrosion process, and establishing the alloying criteria for biological Mg alloys.

(ii) Carrying out an in-depth study on the corrosion properties of biological Mg alloys in simulated body fluids and blood to find out the influencing factors, corrosion mechanism and corrosion laws in the corrosion process, and to provide scientific basis for the development and clinical applications of biological Mg alloys.

(iii) Setting up dynamic simulation environment, simulating the degradation behavior of Mg alloys *in vivo*, and collecting and analyzing *in vivo* experimental data.

Acknowledgments

The authors would also like to thank the Institute of AM of Jiangxi University of Science and Technology.

Funding

This study was supported by the following funds: (1) National Natural Science Foundation of China (51935014, 52165043, 82072084); (2) JiangXi Provincial Natural Science Foundation of China (20212BAB214026); and (3) Jiangsu Provincial Key Research and Development Program (BE2019002).

Conflict of interest

The authors declare that they have no competing financial interests that could have influenced the work reported in this paper.

Author contributions

Conceptualization: Chuyi Liu, Chengrong Ling, and Dongsheng Wang
Funding acquisition: Youwen Yang
Supervision: Youwen Yang and Cijun Shuai
Writing – original draft: Chuyi Liu
Writing – review & editing: Chengrong Ling, Cheng Chen, Youwen Yang, Deqiao Xie, and Cijun Shuai

All authors have read and agreed to the published version of the manuscript.

References

1. Xing F, Li S, Yin D, *et al.*, 2022, Recent progress in Mg-based alloys as a novel bioabsorbable biomaterials for orthopedic applications. *J Magnes Alloys*, 10: 1428–1456.

   https://doi.org/10.1016/j.jma.2022.02.013

2. Tschon M, Boanini E, Sartori M, *et al.*, 2022, Antiosteoporotic nanohydroxyapatite zoledronate scaffold seeded with bone marrow mesenchymal stromal cells for bone regeneration: A 3d *in vitro* model. *Int J Mol Sci*, 23: 5988.

   https://doi.org/10.3390/ijms23115988

3. Xia B, Chen G, 2022, Research progress of natural tissue-derived hydrogels for tissue repair and reconstruction. *Int J Biol Macromol*, 214: 480–491.

   https://doi.org/10.1016/j.ijbiomac.2022.06.137

4. Ni J, Ling H, Zhang S, *et al.,* 2019, Three-dimensional printing of metals for biomedical applications. *Mater Today Bio*, 3: 100024.

   https://doi.org/10.1016/j.mtbio.2019.100024

5. Li J, Qin L, Yang K, *et al.*, 2020, Materials evolution of bone plates for internal fixation of bone fractures: A review. *J Mater Sci Technol*, 36: 190–208.

   https://doi.org/10.1016/j.jmst.2019.07.024

6. Zhang B, Su Y, Zhou J, *et al.*, 2021, Toward a better regeneration through implant-mediated immunomodulation: Harnessing the immune responses. *Adv Sci*, 8: 2100446.

   https://doi.org/10.1002/advs.202100446

7. Bairagi D, Mandal S 2022, A comprehensive review on

biocompatible Mg-based alloys as temporary orthopaedic implants: Current status, challenges, and future prospects. *J Magnes Alloys*, 10: 627–669.

https://doi.org/10.1016/j.jma.2021.09.005

8. Venezuela JJ, Johnston S, Dargusch MS, 2019, The prospects for biodegradable zinc in wound closure applications. *Adv Healthc Mater*, 8: 1900408.

https://doi.org/10.1002/adhm.201900408

9. Kabir H, Munir K, Wen C, *et al.*, 2021, Recent research and progress of biodegradable zinc alloys and composites for biomedical applications: Biomechanical and biocorrosion perspectives. *Bioact Mater*, 6: 836–879.

https://doi.org/10.1016/j.bioactmat.2020.09.013

10. Qin Y, Wen P, Guo H, *et al.*, 2019, Additive manufacturing of biodegradable metals: Current research status and future perspectives. *Acta Biomater*, 98: 3–22.

https://doi.org/10.1016/j.actbio.2019.04.046

11. Venezuela J, Dargusch MS, 2019, The influence of alloying and fabrication techniques on the mechanical properties, biodegradability and biocompatibility of zinc: A comprehensive review. *Acta Biomater*, 87: 1–40.

https://doi.org/10.1016/j.actbio.2019.01.035

12. Shahin M, Wen C, Munir K, *et al.*, 2022, Mechanical and corrosion properties of graphene nanoplatelet-reinforced Mg-Zr and Mg-Zr-Zn matrix nanocomposites for biomedical applications. *J Magnes Alloys*, 10: 458–477.

https://doi.org/10.1016/j.jma.2021.05.011

13. Bommala VK, Krishna MG, Rao CT, 2019, Magnesium matrix composites for biomedical applications: A review. *J Magnes Alloys*, 7: 72–79.

https://doi.org/10.1016/j.jma.2018.11.001

14. Wang JL, Xu JK, Hopkins C, *et al.*, 2020, Biodegradable magnesium-based implants in orthopedics-a general review and perspectives. *Adv Sci*, 7: 1902443.

https://doi.org/10.1002/advs.201902443

15. Chandra G, Pandey A, 2020, Biodegradable bone implants in orthopedic applications: A review. *Biocybern Biomed Eng*, 40: 596–610.

https://doi.org/10.1016/j.bbe.2020.02.003

16. Wu CL, Xie WJ, Man HC, 2022, Laser additive manufacturing of biodegradable Mg-based alloys for biomedical applications: A review. *J Magnes Alloys*, 10: 915–937.

https://doi.org/10.1016/j.jma.2021.12.014

17. Wu S, Liu X, Yeung KW, *et al.*, 2014, Biomimetic porous scaffolds for bone tissue engineering. *Mater Sci Eng R Rep*, 80: 1–36.

https://doi.org/10.1016/j.mser.2014.04.001

18. Yang Y, He C, Dianyu E, *et al.*, 2020, Mg bone implant: Features, developments and perspectives. *Mater Design,* 185: 108259.

https://doi.org/10.1016/j.matdes.2019.108259

19. Li X, Liu X, Wu S, *et al.*, 2016, Design of magnesium alloys with controllable degradation for biomedical implants: From bulk to surface. *Acta Biomater*, 45: 2–30.

https://doi.org/10.1016/j.actbio.2016.09.005

20. Yazdimamaghani M, Razavi M, Vashaee D, *et al.*, 2017, Porous magnesium-based scaffolds for tissue engineering. *Mater Sci Eng C*, 71: 1253–1266.

https://doi.org/10.1016/j.msec.2016.11.027

21. Li C, Guo C, Fitzpatrick V, *et al.*, 2020, Design of biodegradable, implantable devices towards clinical translation. *Nat Rev Mater,* 5: 61–81.

https://doi.org/10.1038/s41578-019-0150-z

22. Malladi L, Mahapatro A, Gomes AS, 2018, Fabrication of magnesium-based metallic scaffolds for bone tissue engineering. *Mater Technol,* 33: 173–182.

https://doi.org/10.1080/10667857.2017.1404278

23. Payr E, 1900, Beitrage zur Technik der Blutgesfass und Nervennaht nebst Mittheilungen die Verwendung eines Resorbierharen Metalles in der Chirurgie. *Arch Klin Chir*, 62: 67–71.

24. Lambotte A, 1909, Technique et indication des protheses dans le traitement des fractures. *Presse Me*d, 17: 321.

25. Mcbride ED, 1938, Absorbable metal in bone surgery: A further report on the use of magnesium alloys. *J Am Med Assoc*, 111: 2464–2467.

https://doi.org/10.1001/jama.1938.02790530018007

26. Witte F, 2010, The history of biodegradable magnesium implants: A review. *Acta Biomater*, 6: 1680–1692.

https://doi.org/10.1016/j.actbio.2010.02.028

27. Biber R, Pauser J, Geßlein M, *et al.*, 2016, Magnesium-based absorbable metal screws for intra-articular fracture fixation. *Case Rep Orthop*, 2016: 9673174.

https://doi.org/10.1155/2016/9673174

28. Chaya A, Yoshizawa S, Verdelis K, *et al.*, 2015, *In vivo* study of magnesium plate and screw degradation and bone fracture healing. *Acta Biomater*, 18: 262–269.

https://doi.org/10.1016/j.actbio.2015.02.010

29. Zhao D, Huang S, Lu F, *et al.*, 2016, Vascularized bone grafting fixed by biodegradable magnesium screw for treating osteonecrosis of the femoral head. *Biomaterials*, 81: 84–92.

https://doi.org/10.1016/j.biomaterials.2015.11.038

30. Wang Z, Sun Z, Han B, *et al.*, 2020, Biological behavior

exploration of a paclitaxel-eluting poly-l-lactide-coated Mg-Zn-Y-Nd alloy intestinal stent *in vivo*. *RSC Adv*, 10: 15079–15090.

https://doi.org/10.1039/C9RA10156J

31. Sing SL, 2022, Perspectives on additive manufacturing enabled beta-titanium alloys for biomedical applications. *Int J Bioprint*, 8: 478.

https://doi.org/10.18063/ijb.v8i1.478

32. Chen Z, Han C, Gao M, *et al.*, 2022, A review on qualification and certification for metal additive manufacturing. *Virtual Phys Prototyp*, 17: 382–405.

https://doi.org/10.1080/17452759.2021.2018938

33. Ng CC, Savalani M, Man HC, 2011, Fabrication of magnesium using selective laser melting technique. *Rapid Prototyp J*, 17: 479–490.

https://doi.org/10.1108/13552541111184206

34. Irrinki H, Nath SD, Alhofors M, *et al.*, 2019, Microstructures, properties, and applications of laser sintered 17-4PH stainless steel. *J Am Ceram Soc*, 102: 5679–5690.

https://doi.org/10.1111/jace.16372

35. Hoeges S, Zwiren A, Schade C, 2017, Additive manufacturing using water atomized steel powders. *Metal Powder Rep*, 72: 111–117.

https://doi.org/10.1016/j.mprp.2017.01.004

36. Moghimian P, Poirié T, Habibnejad-Korayem M, *et al.*, 2021, Metal powders in additive manufacturing: A review on reusability and recyclability of common titanium, nickel and aluminum alloys. *Addit Manuf,* 43: 102017.

https://doi.org/10.1016/j.addma.2021.102017

37. Zheng D, Li Z, Jiang Y, *et al.*, 2022, Effect of multiple thermal cycles on the microstructure evolution of GA151K alloy fabricated by laser-directed energy deposition. *Addit Manuf*, 57: 102957.

https://doi.org/10.1016/j.addma.2022.102957

38. Aboulkhair NT, Simonelli M, Parry L, *et al.*, 2019, 3D printing of aluminium alloys: Additive manufacturing of aluminium alloys using selective laser melting. *Prog Mater Sci*, 106: 100578.

https://doi.org/10.1016/j.pmatsci.2019.100578.

39. Ji X, Mirkoohi E, Ning J, *et al.*, 2020, Analytical modeling of post-printing grain size in metal additive manufacturing. *Opt Lasers Eng*, 124: 105805.

https://doi.org/10.1016/j.optlaseng.2019.105805

40. He C, Bin S, Wu P, *et al.*, 2017, Microstructure evolution and biodegradation behavior of laser rapid solidified Mg-Al-Zn alloy. *Metals*, 7: 105.

https://doi.org/10.3390/met7030105

41. Shuai C, Yang Y, Wu P, *et al.*, 2017, Laser rapid solidification improves corrosion behavior of Mg-Zn-Zr alloy. *J Alloys Compd*, 691: 961–969.

https://doi.org/10.1016/j.jallcom.2016.09.019

42. Spierings AB, Dawson K, Dumitraschkewitz P, *et al.*, 2018, Microstructure characterization of SLM-processed Al-Mg-Sc-Zr alloy in the heat treated and HIPed condition. *Addit Manuf*, 20: 173–181.

https://doi.org/10.1016/j.addma.2017.12.011

43. Buhairi MA, Foudzi FM, Jamhari FI, *et al.*, 2022, Review on volumetric energy density: Influence on morphology and mechanical properties of Ti6Al4V manufactured via laser powder bed fusion. *Prog Addit Manuf*,

https://doi.org/10.1007/s40964-022-00328-0

44. Liang J, Lei Z, Chen Y, *et al.*, 2022, Formability, microstructure, and thermal crack characteristics of selective laser melting of ZK60 magnesium alloy. *Mater Sci Eng A*, 839: 142858.

https://doi.org/10.1016/j.msea.2022.142858

45. Esmaily M, Zeng Z, Mortazavi AN, *et al.*, 2020, A detailed microstructural and corrosion analysis of magnesium alloy WE43 manufactured by selective laser melting. *Addit Manuf*, 35: 101321.

https://doi.org/10.1016/j.addma.2020.101321

46. Wei K, Gao M, Wang Z, Zeng X, 2014, Effect of energy input on formability, microstructure and mechanical properties of selective laser melted AZ91D magnesium alloy. *Mater Sci Eng A*, 611: 212–222.

https://doi.org/10.1016/j.msea.2014.05.092

47. Yang Y, Wu P, Lin X, *et al.*, 2016, System development, formability quality and microstructure evolution of selective laser-melted magnesium. *Virtual Phys Prototyp*, 11: 173–181.

https://doi.org/10.1080/17452759.2016.1210522

48. Sezer N, Evis Z, Koç M, 202, Additive manufacturing of biodegradable magnesium implants and scaffolds: Review of the recent advances and research trends. *J Magnes Alloys*, 9: 392–415.

https://doi.org/10.1016/j.jma.2020.09.014

49. Liu S, Yang W, Shi X, *et al.*, 2019, Influence of laser process parameters on the densification, microstructure, and mechanical properties of a selective laser melted AZ61 magnesium alloy. *J Alloys Compd*, 808: 151160.

https://doi.org/10.1016/j.jallcom.2019.06.261

50. Liu C, Zhang M, Chen C, 2017, Effect of laser processing parameters on porosity, microstructure and mechanical properties of porous Mg-Ca alloys produced by laser additive manufacturing. *Mater Sci Eng A*, 703: 359-371.

https://doi.org/10.1016/j.msea.2017.07.031

51. Yang Y, Lu C, Peng S, *et al.*, 2020, Laser additive manufacturing of Mg-based composite with improved degradation behaviour. *Virtual Phys Prototyp*, 15: 278–293.

    https://doi.org/10.1080/17452759.2020.1748381

52. Zhang M, Chen C, Liu C, *et al.*, Study on porous Mg-Zn-Zr ZK61 alloys produced by laser additive manufacturing. *Metals*, 8: 635.

    https://doi.org/10.3390/met8080635

53. Deng Q, Wu Y, Wu Q, *et al.*, 2022, Microstructure evolution and mechanical properties of a high-strength Mg-10Gd-3Y-1Zn-0.4Zr alloy fabricated by laser powder bed fusion. *Addit Manuf*, 49: 102517.

    https://doi.org/10.1016/j.addma.2021.102517

54. Wang T, Meng Q, Araby S, *et al.*, 2021, Non-oxidized graphene/metal composites by laser deposition additive manufacturing. *J Alloys Compd,* 882: 160724.

    https://doi.org/10.1016/j.jallcom.2021.160724

55. Cao X, Jahazi M, Immarigeon JP, *et al.*, 2006, A review of laser welding techniques for magnesium alloys. *J Mater Process Technol*, 171: 188–204.

    https://doi.org/10.1016/j.jmatprotec.2005.06.068

56. Manakari V, Parande G, Gupta M, 2017, Selective laser melting of magnesium and magnesium alloy powders: A review. *Metals*, 7: 2.

    https://doi.org/10.3390/met7010002

57. Gangireddy S, Gwalani B, Liu K, *et al.*, 2019, Microstructure and mechanical behavior of an additive manufactured (AM) WE43-Mg alloy. *Addit Manuf*, 26: 53–64.

    https://doi.org/10.1016/j.addma.2018.12.015

58. Hosseini E, Popovich VA, 2019, A review of mechanical properties of additively manufactured Inconel 718. *Addit Manuf*, 30: 100877.

    https://doi.org/10.1016/j.addma.2019.100877

59. Wang Y, Fu P, Wang N, *et al.*, 2020, Challenges and solutions for the additive manufacturing of biodegradable magnesium implants. *Engineering*, 6: 1267–1275.

    https://doi.org/10.1016/j.eng.2020.02.015

60. Dou Y, Cai S, Ye X, *et al.*, 2013, 45S5 bioactive glass-ceramic coated AZ31 magnesium alloy with improved corrosion resistance. *Surf Coat Technol*, 228: 154–161.

    https://doi.org/10.1016/j.surfcoat.2013.04.022

61. Rojaee R, Fathi M, Raeissi K 2013, Electrophoretic deposition of nanostructured hydroxyapatite coating on AZ91 magnesium alloy implants with different surface treatments. *Appl Surf Sci*, 285: 664–673.

    https://doi.org/10.1016/j.apsusc.2013.08.108

62. Razavi M, Fathi M, Savabi O, *et al.*, 2014, Controlling the degradation rate of bioactive magnesium implants by electrophoretic deposition of akermanite coating. *Ceram Int*, 40: 3865–3872.

    https://doi.org/10.1016/j.ceramint.2013.08.027

63. Kopp A, Derra T, Müther M, *et al.*, 2019, Influence of design and postprocessing parameters on the degradation behavior and mechanical properties of additively manufactured magnesium scaffolds. *Acta Biomater*, 98: 23–35.

    https://doi.org/10.1016/j.actbio.2019.04.012

64. Han J, Chen J, Peng L, *et al.*, 2017, Microstructure, texture and mechanical properties of friction stir processed Mg-14Gd alloys. *Mater Design*, 130: 90–102.

    https://doi.org/10.1016/j.matdes.2017.05.046

65. Huang C, Yan X, Zhao L, *et al.*, 2019, Ductilization of selective laser melted Ti6Al4V alloy by friction stir processing. *Mater Sci Eng A*, 755: 85–96.

    https://doi.org/10.1016/j.msea.2019.03.133

66. Macías JG, Elangeswaran C, Zhao L, *et al.*, 2019, Ductilisation and fatigue life enhancement of selective laser melted AlSi10Mg by friction stir processing. *Scr Mater*, 170: 124–128.

    https://doi.org/10.1016/j.scriptamat.2019.05.044

67. Deng Q, Wu Y, Su N, *et al.*, 2021, Influence of friction stir processing and aging heat treatment on microstructure and mechanical properties of selective laser melted Mg-Gd-Zr alloy. *Addit Manuf*, 44: 102036.

    https://doi.org/10.1016/j.addma.2021.102036

68. Alfieri V, Argenio P, Caiazzo F, *et al.*, 2017, Reduction of surface roughness by means of laser processing over additive manufacturing metal parts. *Materials*. 10: 30.

    https://doi.org/10.3390/ma10010030

69. Basha SM, Bhuyan M, Basha MM, *et al.*, 2020, Laser polishing of 3D printed metallic components: A review on surface integrity. *Mater Today Proc*, 26: 2047–2054.

    https://doi.org/10.1016/j.matpr.2020.02.443

70. Zhang X, Li XW, Li JG, *et al.*, 2014, Preparation and mechanical property of a novel 3D porous magnesium scaffold for bone tissue engineering. *Mater Sci Eng C*, 42: 362–367.

    https://doi.org/10.1016/j.msec.2014.05.044

71. Hyer H, Zhou L, Benson G, *et al.*, 2020, Additive manufacturing of dense WE43 Mg alloy by laser powder bed fusion. *Addit Manuf*, 33: 101123.

    https://doi.org/10.1016/j.addma.2020.101123

72. Fang X, Yang J, Wang S, *et al.*, 2022, Additive manufacturing of high performance AZ31 magnesium alloy with full equiaxed grains: Microstructure, mechanical property, and electromechanical corrosion performance. *J Mater Proc*

Technol, 300: 117430.

https://doi.org/10.1016/j.jmatprotec.2021.117430

73. Wang Y, Huang H, Jia G, *et al.*, 2021, Fatigue and dynamic biodegradation behavior of additively manufactured Mg scaffolds. *Acta Biomater*, 135: 705–722.

https://doi.org/10.1016/j.actbio.2021.08.040

74. Chen J, Wu P, Wang Q, *et al.*, 2016, Influence of alloying treatment and rapid solidification on the degradation behavior and mechanical properties of Mg. *Metals*, 6: 259.

https://doi.org/10.3390/met6110259

75. Liu J, Liu B, Min S, *et al.*, 2022, Biodegradable magnesium alloy WE43 porous scaffolds fabricated by laser powder bed fusion for orthopedic applications: Process optimization, *in vitro* and *in vivo* investigation. *Bioact Mater*, 16: 301–319.

https://doi.org/10.1016/j.bioactmat.2022.02.020

76. Hyer H, Zhou L, Liu Q, *et al.*, 2021, High strength WE43 microlattice structures additively manufactured by laser powder bed fusion. *Materialia*, 16: 101067.

https://doi.org/10.1016/j.mtla.2021.101067

77. Zhang WN, Wang LZ, Feng ZX, *et al.*, 2020, Research progress on selective laser melting (SLM) of magnesium alloys: A review. *Optik*, 207: 163842.

https://doi.org/10.1016/j.ijleo.2019.163842

78. Shuai C, Li S, Peng S, *et al.*, 2019, Biodegradable metallic bone implants. *Mater Chem Front*, 3: 544–562.

https://doi.org/10.1039/C8QM00507A

79. Liu J, Lin Y, Bian D, *et al.*, 2019, *In vitro* and *in vivo* studies of Mg-30Sc alloys with different phase structure for potential usage within bone. *Acta Biomater*, 98: 50–66.

https://doi.org/10.1016/j.actbio.2019.03.009

80. Han HS, Loffredo S, Jun I, *et al.*, 2019, Current status and outlook on the clinical translation of biodegradable metals. *Mater Today*, 23: 57–71.

https://doi.org/10.1016/j.mattod.2018.05.018

81. Cao F, Shi Z, Song GL, *et al.*, 2013, Corrosion behaviour in salt spray and in 3.5% NaCl solution saturated with Mg(OH)2 of as-cast and solution heat-treated binary Mg-X alloys: X=Mn, Sn, Ca, Zn, Al, Zr, Si, Sr. *Corros Sci*, 76: 60–97.

https://doi.org/10.1016/j.corsci.2013.06.030

82. Peng Q, Huang Y, Zhou L, *et al.*, 2010, Preparation and properties of high purity Mg-Y biomaterials. *Biomaterials*, 31: 398–403.

https://doi.org/10.1016/j.biomaterials.2009.09.065

83. Shuai S, Guo E, Zheng Q, *et al.*, 2016, Three-dimensional α-Mg dendritic morphology and branching structure transition in Mg-Zn alloys. *Mater Charact*, 118: 304–308.

https://doi.org/10.1016/j.matchar.2016.06.009

84. Li J, Xie D, Yu H, *et al.*, 2020, Microstructure and mechanical property of multi-pass low-strain rolled Mg-Al-Zn-Mn alloy sheet. *J Alloys Compd*, 835: 155228.

https://doi.org/10.1016/j.jallcom.2020.155228

85. Luo Q, Guo Y, Liu B, *et al.*, 2020, Thermodynamics and kinetics of phase transformation in rare earth-magnesium alloys: A critical review. *J Mater Sci Technol*, 44: 171–190.

https://doi.org/10.1016/j.jmst.2020.01.022

86. Leleu S, Rives B, Bour J, *et al.*, 2018, On the stability of the oxides film formed on a magnesium alloy containing rare-earth elements. *Electrochim Acta,* 290: 586–594.

https://doi.org/10.1016/j.electacta.2018.08.093

87. Willbold E, Gu X, Albert D, *et al.*, 2015, Effect of the addition of low rare earth elements (lanthanum, neodymium, cerium) on the biodegradation and biocompatibility of magnesium. *Acta Biomater*, 11: 554–562.

https://doi.org/10.1016/j.actbio.2014.09.041

88. Wang C, Shuai Y, Yang Y, *et al.*, 2022, Amorphous magnesium alloy with high corrosion resistance fabricated by laser powder bed fusion. *J Alloys Compd*, 897: 163247.

https://doi.org/10.1016/j.jallcom.2021.163247

89. Chen S, Tu J, Hu Q, *et al.*, 2017, Corrosion resistance and *in vitro* bioactivity of Si-containing coating prepared on a biodegradable Mg-Zn-Ca bulk metallic glass by micro-arc oxidation. *J Non Cryst Solids*, 456: 125–131.

https://doi.org/10.1016/j.jnoncrysol.2016.11.011

90. Zhang D, Qin Y, Feng W, *et al.*, 2019, Microstructural evolution of the amorphous layers on Mg-Zn-Ca alloy during laser remelting process. *Surf Coat Technol*, 363: 87–94.

https://doi.org/10.1016/j.surfcoat.2019.02.051

91. Zberg B, Arata ER, Uggowitzer PJ, *et al.*, 2009, Tensile properties of glassy MgZnCa wires and reliability analysis using Weibull statistics. *Acta Mater*, 57: 3223–3231.

https://doi.org/10.1016/j.actamat.2009.03.028

92. Shuai C, Liu L, Zhao M, *et al.*, 2018, Microstructure, biodegradation, antibacterial and mechanical properties of ZK60-Cu alloys prepared by selective laser melting technique. *J Mater Sci Technol*, 34: 1944–1952.

https://doi.org/10.1016/j.jmst.2018.02.006

93. Spriano S, Yamaguchi S, Baino F, *et al.*, 2018, A critical review of multifunctional titanium surfaces: New frontiers for improving osseointegration and host response, avoiding bacteria contamination. *Acta Biomater*, 79: 1–22.

https://doi.org/10.1016/j.actbio.2018.08.013

94. Ouyang P, Dong H, He X, *et al.*, 2019, Hydromechanical mechanism behind the effect of pore size of porous titanium scaffolds on osteoblast response and bone ingrowth. *Mater Design*, 183: 108151.

https://doi.org/10.1016/j.matdes.2019.108151

95. Rojaee R, Fathi M, Raeissi K, 2013, Controlling the degradation rate of AZ91 magnesium alloy via sol-gel derived nanostructured hydroxyapatite coating. *Mater Sci Eng C*, 33: 3817–3825.

https://doi.org/10.1016/j.msec.2013.05.014

96. Tian M, Cai S, Ling L, *et al.*, 2022, Superhydrophilic hydroxyapatite/hydroxypropyltrimethyl ammonium chloride chitosan composite coating for enhancing the antibacterial and corrosion resistance of magnesium alloy. *Prog Org Coat*, 165: 106745.

https://doi.org/10.1016/j.porgcoat.2022.106745

97. Roshan NR, Hassannejad H, Nouri A, 2021, Corrosion and mechanical behaviour of biodegradable PLA-cellulose nanocomposite coating on AZ31 magnesium alloy. *Surf Eng*, 37: 236–245.

https://doi.org/10.1080/02670844.2020.1776093

98. Dutta S, Devi KB, Mandal S, *et al.,* 2019, *In vitro* corrosion and cytocompatibility studies of hot press sintered magnesium-bioactive glass composite. *Materialia*, 5: 100245.

https://doi.org/10.1016/j.mtla.2019.100245

99. Kang YG, Wei J, Shin JW, *et al.*, 2018, Enhanced biocompatibility and osteogenic potential of mesoporous magnesium silicate/polycaprolactone/wheat protein composite scaffolds. *Int J Nanomed*, 13: 1107–1117.

https://doi.org/10.2147/ijn.S157921

100. Gong X, Zeng D, Groeneveld-Meijer W, *et al.*, 2022, Additive manufacturing: A machine learning model of process-structure-property linkages for machining behavior of Ti-6Al-4V. *Mater Sci Addit Manuf*, 1: 6.

https://doi.org/10.18063/msam.v1i1.6

101. Sing SL, Kuo CN, Shih CT, *et al.*, 2021, Perspectives of using machine learning in laser powder bed fusion for metal additive manufacturing. *Virtual Phys Prototyp*, 16: 372–386.

https://doi.org/10.1080/17452759.2021.1944229